Numerical analyses of baseline JT-60SA design concepts with the COREDIV code

R. Zagórski[1], K.Gałązka[1], I. Ivanova-Stanik[1], W.Stępniewski[1], L.Garzotti[2], G.Giruzzi[3], R.Neu[4] and M.Romanelli[2]

[1]Institute of Plasma Physics and Laser Microfusion, Hery Str. 23, 01-497 Warsaw, Poland

[2]CCFE, Culham Science Centre, Abingdon, Oxon, OX14 3DB, UK

[3]CEA, IRFM, F-13108 Saint-Paul-lez-Durance, France

[4]Max-Planck Institut für Plasmaphysik, 85748 Garching, Germany

E-mail contact of main author: roman.zagorski@ipplm.pl

Abstract. JT-60SA reference design scenarios at high (#3) and low (#2) density have been analyzed with the help of the self-consistent COREDIV code. Simulations results for standard carbon wall and the full W have been compared in terms of the influence of impurities, both intrinsic (C, W) and seeded (N, Ar, Ne, Kr) on the radiation losses and plasma parameters. For the scenario #3 in carbon environment the regime of detachment on divertor plates can be achieved with N or Ne seeding, whereas for the low density and high power scenario (#2), the carbon and seeding impurity radiation does not effectively reduce power to the targets. In this case only increase of neither average density or edge density together with Kr seeding might help to develop conditions with strong radiation losses and semi-detached conditions in the divertor. The calculations show that in case of tungsten divertor the power load to the plate is mitigated by seeding and the central plasma dilution is smaller compared to the carbon divertor. For the high density case with neon seeding operation in full detachment mode is observed. Ar seems to be an optimal choice for the low density high power scenario #2, showing wide operating window, whereas Ne leads to high plasma dilution at high seeding levels albeit not achieving semi-detached conditions in the divertor.

1. Introduction

JT-60SA is a superconducting tokamak supporting thermonuclear fusion research on the way towards realization of energy production in a DEMO reactor. It will complement ITER in resolving some key engineering and physics issues for DEMO operation[1]. The baseline JT-60SA design foresees full carbon wall, however feasibility studies have been initiated recently to assess the possibility of the transition to full W environment in the extended phase of the JT-60SA operation. According to engineering limits for ITER, the maximum heat dissipated at the divertor plate has to be lower than 10 M W/m^2 in steady state [2]. This can be achieved by radiative cooling in the pedestal and scrape-off layer (SOL) areas, which helps to spread the energy over a larger area and to reduce the energy flux towards the target. Effective radiating cooling can be provided by seeded or intrinsic impurities. The influence of various seeding gases on the improvement of energy confinement on JT-60U has been already extensively investigated experimentally and numerically. For instance in Ne-seeded discharges neon was found to contribute the dominant part of radiation during detachment [3]. In this paper, JT-60SA reference design scenarios [1] at high (#3) and low (#2) density have been analyzed with the help of the self-consistent core-edge COREDIV code [4]. COREDIV is able to investigate tokamak plasmas with various divertor plate materials as well as various seeded impurities [5-10]. Simulation results for the standard carbon wall [11] and the planned full tungsten configuration have been compared in terms of the influence of impurities, both intrinsic (C, W) and seeded (N, Ar, Ne, Kr) on the radiation losses and plasma parameters. In particular, the reduction of the divertor target power load due to radiation of sputtered and externally seeded impurities has been investigated.

2. Model Description

The physical model used in the COREDIV code is based on a self-consistent coupling of the 1D transport in the core to the 2D multifluid description of the scrape-off layer and has been already presented elsewhere [4, 11, 12]. Although the device geometry and treatment of neutral particles is simplified, the code can produce quantitative agreement with experimental observations in a time-efficient manner. The code has been already successfully benchmarked with a number of JET discharges, including the nitrogen seeded type I and type III ELMy H-mode discharges [6, 8, 9] and recently, JET ILW configuration [10]. COREDIV has also been applied to ASDEX Upgrade (AUG) discharges in the full W environment [7].

In the core, the 1D radial transport equations for bulk ions, for each ionization state of impurity ions and for the electron and ion temperature are solved. It is assumed that all ions have the same temperature. Parabolic-like deposition profile is assumed for auxiliary heating. The energy losses are determined by bremsstrahlung, synchrotron and line radiation. The equation for the poloidal magnetic field has been neglected and thus the current distribution is assumed to be given in our approach.

The electron and ion energy fluxes are defined by the local transport model proposed in Ref.[13] which reproduces a prescribed energy confinement law. In particular, the anomalous heat conductivity is given by the expression $\chi_{e,i} = C_{e,i} \frac{a^2}{\tau_E} \left[1 + \left(\frac{r}{a} \right)^4 \right] F(r)$ where τ_E is the energy confinement time defined by the ELMy H-mode scaling law, a is the plasma radius and the coefficients C_e, C_i, ($C_e = 2C_i$) are adjusted to have agreement between calculated and experimental confinement times. The parabolic like profile function $F(r)$ is modified to provide transport barrier in the plasma edge with the barrier width of about 5 cm which results in the plasma temperature at the pedestal of the order of 1.2-1.5 keV. It should be stressed that the simplified transport model presented here does not aim on detailed transport predictions for JT60-SA scenarios as done for example in the recent papers of J.Garcia [14] and G.Giruzzi [15]. It is important only that the model reflects the main findings of the more sophisticated transport descriptions like GLF23 or CDBM in terms of the global confinement time and pedestal characteristics. It should be stressed however, that the COREDIV predictions related to the investigations of the impurity influence on the discharge parameters are not very much sensitive to the details of the profiles of the transport coefficients.

The profile of the main plasma ion density is given by the solution of the radial diffusion equation with diffusion coefficients $D_e = D_i = 0.1\chi_e$ and the source term taking into account the attenuation of the neutral density due to ionization processes. The source intensity is determined by the internal iteration procedure in such a way that the average electron density obtained from the neutrality condition equals to that of the scenario considered. The radial impurity transport is described by standard neoclassical (collisionality dependent) with small contribution from the anomalous transport. The neoclassical impurity transport is based on large aspect ratio assumption and includes both, the diffusion term and the pinch velocity due to density and temperature gradients (off-diagonal terms) corresponding to the contributions from Pfirsch-Schlüter and banana-plateau collisionality regimes. However, for tungsten transport simulations only anomalous contribution has been considered to avoid tungsten accumulation in the core.

In the SOL we use the 2D boundary layer description [16,17], which like most other 2D computational plasma edge fluid models is primarily based on the classical Braginskii [18]. transport equations. The transport along field lines is assumed to be classical, whereas radial transport is anomalous with prescribed radial transport coefficients. For deuterium ions and for each ionization state of each impurity species we solve the continuity and parallel momentum equations. In addition, two energy equations for electron temperature (T_e) and for

one common ion temperature (T_i) are solved. A simplified neutral model is considered in order to avoid time consuming Monte Carlo iterations. It allows however, the inclusion of plasma recycling as well as the sputtering processes at the target plates. We assume that the divertor is in attached (semi-attached) mode that the ratio between electron separatrix density and volume average density is kept constant in our simulations (usually $n_{es} = 0.4\, n_e$). In order to keep the prescribed plasma density at the separatrix (at stagnation point), the deuterium recycling coefficient ($0 < R_H < 1$) was iterated accordingly. The energy losses due to interactions with hydrogenic atoms (line radiation, ionization and charge exchange) are accounted for in the model. Although the temperature usually is high at the strike points and, as a consequence, physical sputtering is the dominant mechanism for impurity release, also the contribution of chemical sputtering of carbon is considered. The radial transport in the SOL is fixed with radial diffusion $D_{SOL} = 0.5\ m^2/s$, $\chi_e = 1\ m^2/s$, $\chi_i = 0.5\ m^2/s$. The standard sheath boundary conditions are imposed at the plates, whereas at the wall the boundary conditions are given by decay lengths. The parallel velocities and the gradients of densities and temperatures are assumed to be zero at the midplane (stagnation point) and at the interface with the private region which is not accounted for in our model. The coupling between the core and the SOL is made by imposing continuity of energy and particle fluxes as well as of particle densities and temperatures at the separatrix. In the COREDIV code the description of the transport in the core and SOL region is simplified as the main aim is to analyze the influence of the impurities on the radiative heat losses, divertor target load and impurity concentrations. However, one has to take into account the limitations of the model resulting from the assumptions, for instance no implemented treatment of ELM's. Therefore, all the COREDIV results should be interpreted as time-averaged quantities [9].

2.1. Modeled scenarios

In our work we focus on two JT-60SA inductive scenarios: #2 with low density ($n_e=5.6x10^{19}\ m^{-3}$) high heating power ($P_{aux}=41\ MW$) and #3 with high density ($n_e=9x10^{19}\ m^{-3}$) and moderate auxiliary power ($P_{aux}=30\ MW$). Simulations aim at comparison of the standard full carbon (C) configuration with the planned full tungsten (W) environment in terms of the influence of impurities, both intrinsic (C, W) and seeded nitrogen (N), neon (Ne), argon (Ar) and krypton (Kr) on the radiation losses and plasma parameters. In particular, the reduction of the divertor target power load due to radiation of sputtered and externally seeded impurities has been investigated. The main focus is to study the stationary state achieved for different gas seeding levels. As the reference input parameters, we consider $D_{SOL} = 0.5\ m^2/s$ and $n_{es}=0.4\ n_e$. However, the influence of changes to these parameters (radial diffusion coefficient in the SOL and electron density at separatrix) on the stationary state is analysed too. In particular, the total impurity concentrations, radiation losses and corresponding heat loads at the target are calculated. Due to the fact that in #3 the density is higher and the auxiliary power lower than in #2, N or Ne are able to provide enough cooling and therefore simulations with other seeding impurities are omitted. The main aim of our studies of JT-60SA scenarios[1] was to check whether highly radiating plasmas with strong mitigation of the heat loads can be achieved. The most important tool to realize this goal should be impurity seeding, which is expected to lead to strong edge radiation and mitigation the erosion of target material.
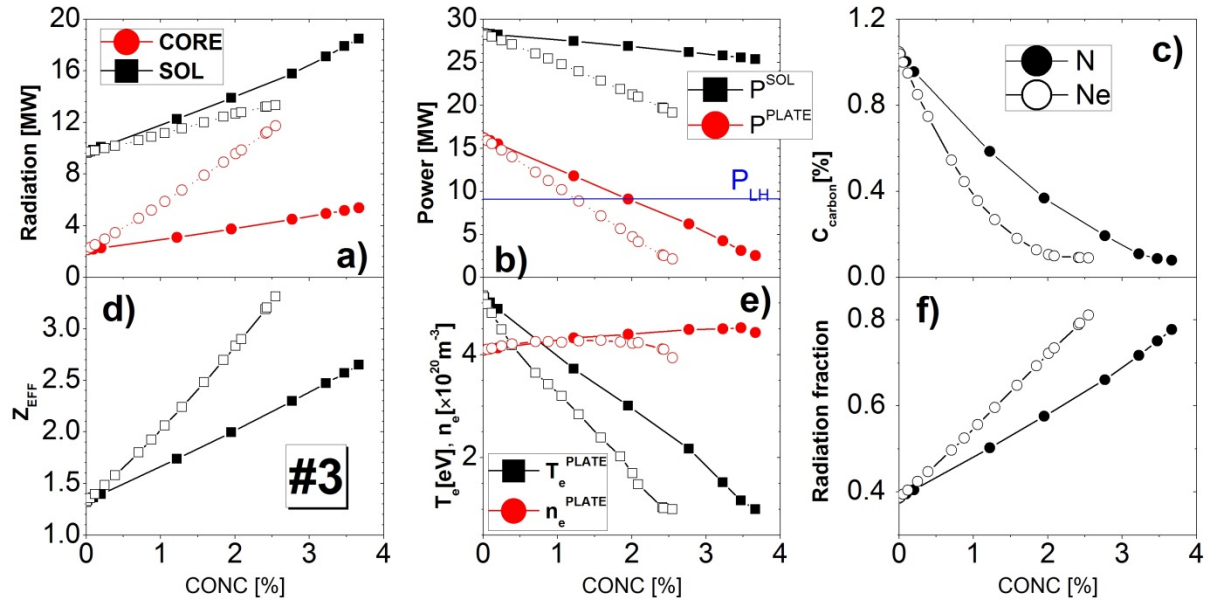
FIG.1: *Plasma parameters for scenario #3 with C PFCs versus N (full symbols) and Ne (open symbols) concentrations: a) core and SOL radiation; b) Power to plate P^{PLATE} and to the SOL (P^{SOL}); c) C concentration in the core; d) Z_{eff}; e) n_e and T_e at the strike point; f) radiation fraction (f_{rad}).*

2.2. Simulations of JT-60SA scenarios with C wall

For the high density scenario (#3) as well as for low density one (#2), calculations have been performed assuming N and Ne as the reference seeding gases, which appeared to be quite successful in experiments on AUG and JET with carbon and W walls [6-7]. However, for the low density scenario (#2) seeding by other gasses (Ar, Kr) has been investigated as well. It has been found that all the main plasma parameters of analysed scenarios can be reasonably reproduced by COREDIV simulations [11].
. It should be noted, that for considered scenarios for cases without seeding the power load to target plates is relatively high (*>16 MW*) showing that JT-60SA can work in a power density range of great interest for DEMO. However, to reduce the heat load to the divertor, plasma seeding seems to be an unavoidable requirement for the high power long pulse discharges. We point out, that due to the limitations of the model (slab geometry, target perpendicular to the field lines, symmetric divertor) it is impossible to give the correct value of the peak heat flux to the target and therefore in the figures we present only the total power to divertor plates. In the Fig.1, we show the main plasma parameters for the high density scenario #3 versus impurity concentrations for N and Ne seeding for C PFCs. It appears that for this scenario, low Z impurity seeding (N, Ne) leads to the increased plasma radiation (*f_{rad} ~80%*, Fig.1f) and strong reduction of the power load to the divertor plates. The reduction of P^{PLATE} is mostly due to the increased N or Ne radiation (with increased puffing), for N mostly from the divertor region whereas for Ne also from the core (Figs.1a). For the highest seeding levels, plasma detachment in the divertor can be approached, simultaneously with the reasonable level of the plasma contamination, which however is higher for Ne. It is achieved thanks to both, the good screening efficiency of the SOL plasma for this high density discharge and due to replacement of the carbon ions by nitrogen/neon; carbon erosion is almost completely mitigated for large seeding levels (Fig.1c).

In the case of the low density, high power scenario (#2) the situation is different as it can be seen from the Fig.2, where the main plasma parameters are shown versus the N concentration. N seeding leads to moderate plasma radiation ($f_{rad} \sim 60\%$) but simultaneously $Z_{eff} \sim 6$ is very high and strong plasma dilution
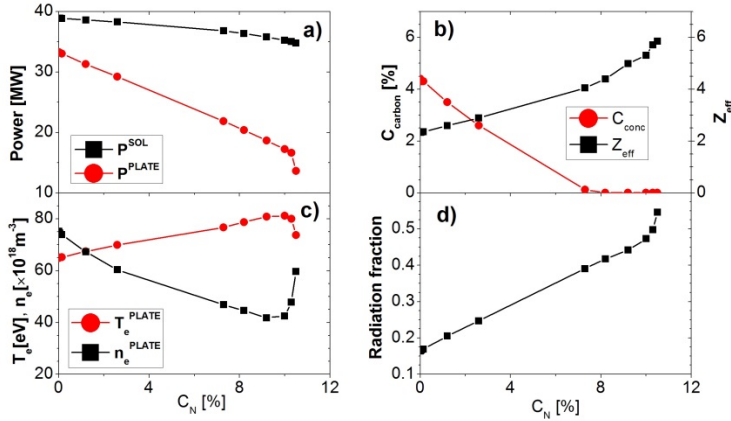

FIG.2: Plasma parameters for scenario #2 with C PFCs versus impurity concentrations for N seeding: a) Power to plate and to the SOL; b) carbon concentration in the core and Z_{eff}; c) n_e and T_e at the plate (strike point); d) radiation fraction.

is obtained. In addition the divertor conditions are far from plasma detachment with very high temperature ($T_e > 60\ eV$) and low plasma density at the strike point. In spite of this high plasma temperature (and corresponding significant C erosion), the C concentration in the core plasma is negligible, which is the effect of the very good screening of the C ions in the case of this strongly seeded plasmas. It should be noted, that even for the highest seeding the power to the target plates might be relatively high (> 14MW). In order to check how the situation can be improved, simulations with other seeding gasses have been performed. We have considered in addition to N also Ne, Ar and Kr seeding. Some plasma parameters versus the seeding impurity concentration are shown in the Fig.3.
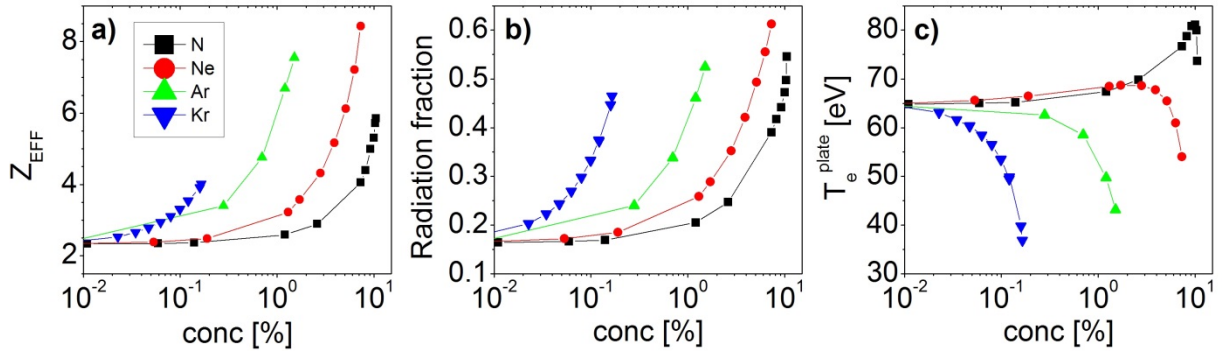

FIG. 3: Plasma parameters for scenario #2 versus concentrations of seeding gases (N, Ne, Ar and Kr): a) Z_{eff}; b) radiation fraction; c) T_{plate} at strike point

It appears that the situation cannot be improved much with other gasses, and a radiation fraction higher than 60% cannot be achieved. Simultaneously the highest radiation is achieved at high plasma dilution with strike point temperatures very high. It has been found that for the low Z seeding gasses (N, Ne) the solution is limited by the plasma dilution, whereas for high Z gases (Ar, Kr) radiative collapse is the limiting process. Ne and N radiate well in edge region but with high Z_{eff}, whereas Kr gives the lowest Z_{eff} and radiates mostly in the core. However, Kr seeding might be an interesting option for high power shots with slightly higher plasma average or edge density as it can be seen in Fig.4, where comparison for scenario #2 is shown for different average and edge densities: the reference one $n_e = 5.6 \times 10^{19}\ m^{-3}$, $n_{es} = 0.4 n_e$ and higher plasma density ($n_e = 7.5 \times 10^{19}\ m^{-3}$) or edge density $n_{es} == 0.6 n_e$. A highly radiative plasma is clearly achievable for the higher densities, mostly due to the strong krypton radiation in the core leading to overall radiation losses up to 73% (Fig.4a) and reduced power to the divertor ($P^{PLATE} \sim 7 - 8MW$) at a reasonable level of plasma

contamination ($Z_{eff} \sim 3.5$) and reduced carbon erosion. Simultaneously the power crossing separatrix remains above the H-L transition threshold ($P^{SOL} > 18MW$). The temperature in the divertor is low (Fig.4b) and the plasma density high, indicating the possibility of the achievement of a semi-detached state in the divertor region.

3. Results for W divertor

It has been found that in both scenarios with W divertor the power delivered to the divertor plate without seeding is very high and using a seeding gas to control energy exhaust is indispensable. That conclusion remains valid independent on the assumptions regarding the edge radial transport or edge density values. Calculations done for scenario #3 with Ne seeding and for the reference input parameters (Sec.2.1) show existence of very wide
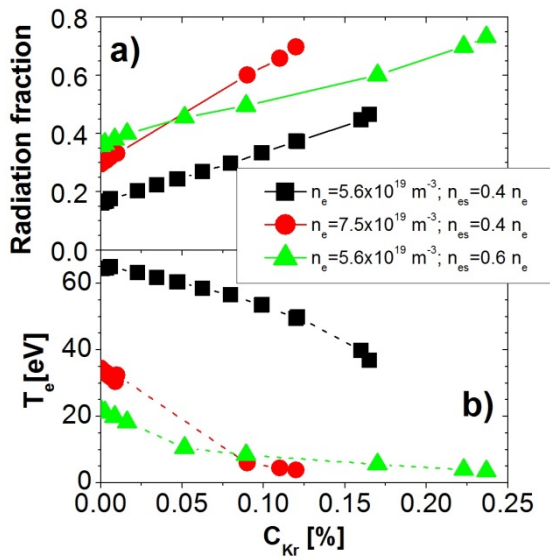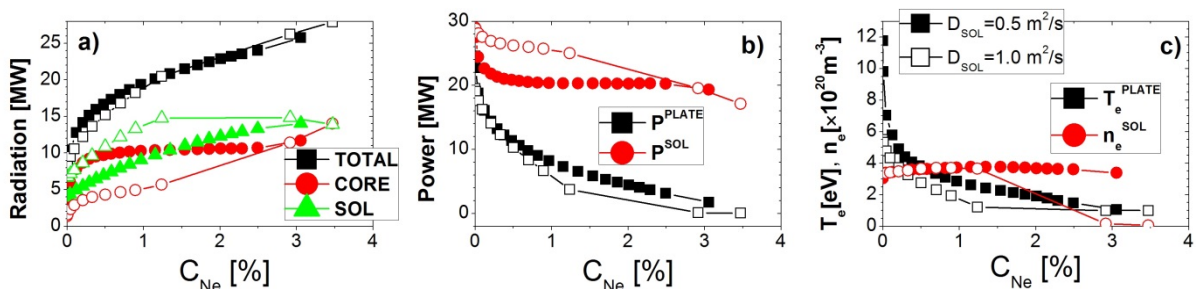

FIG. 4: Plasma parameters for scenario #2 with C PFCs and for different plasma densities versus Kr concentration: a) radiation fraction; b) T_e at the strike point.

operating window, since already for relatively low Ne concentrations ($C_{Ne} > 0.7\%$) the divertor heat load is below the technological limit requirements (*10 MW/m²*, assuming *1 m²* of divertor wetting area) whereas the power crossing the separatrix stays above the P_{L-H} power threshold (see Fig.5). The energy losses are dominated by Ne and deuterium radiation and for maximum applied seeding ($C_{Ne} = 3.1\%$) up to 83% of the input power can be radiated with 17.2 MW of Ne radiation and with negligible W radiation. Simultaneously the electron temperature at the divertor target is low (~ 1 eV) indicating semi-detached conditions (Fig.5). This rather optimistic result has been further analyzed in terms of different plasma edge parameters (eg. separatrix density, radial anomalous transport). In line with our earlier simulations for JET-ILW [19] and ITER [20] also in the case of JT-60SA it has been found that the

increased radial diffusion ($D_{SOL} = 1$ m²/s, open symbols in Fig.5) improves the impurity retention in the SOL leading to the increased divertor radiation losses and easier access of detachment. Similar effect on the results has the increased edge density.

In Fig.6, simulation results are shown for the #2 with tungsten wall and Ne, Ar, and Kr seeding for our reference input parameters (Sec.2.1). It can be seen, that in contrast to the situation with carbon environment, this time seeding by all considered impurities leads to the efficient mitigation of the power flux to the target plates as well as to the reduction of the tungsten production and radiation.

FIG.5: Plasma parameters for scenario #3 in W environment versus Ne core concentration: a) total, core and SOL radiation; b) power to divertor plates and to the SOL ; c) n_e and T_e at the strike point.

Already at reasonable levels of plasma contamination $C_{Ne} \geq 1.5$ % ($Z_{eff} \geq 3$), $C_{Ar} \geq 0.3$ % ($Z_{eff} \geq 2.5$), $C_{Kr} \geq 0.1$ % ($Z_{eff} \geq 2.6$), the power load to the target is reduced below 10 MW, with the power crossing separatrix still above the P_{L-H} threshold. Simultaneously, the plate temperature is low ($T_e^{plate} \leq 7.5$ eV), but only Ar and Kr seeding leads to high plasma density in the divertor, whereas for Ne the strong plasma dilution at highest seeding levels prevents
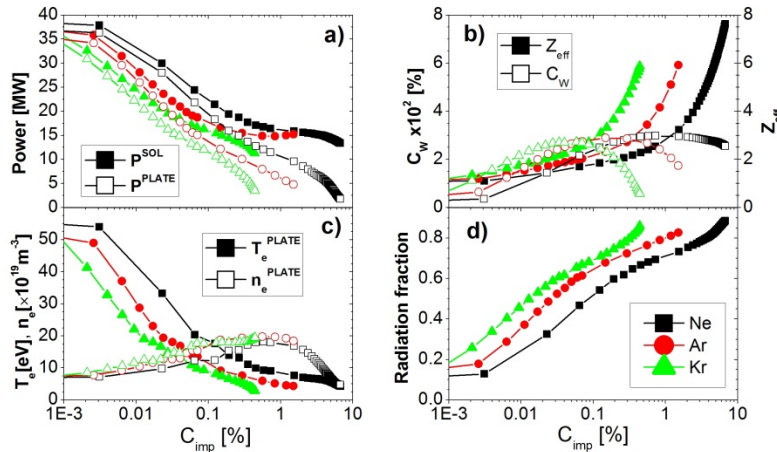

FIG. 6: Plasma parameters for scenario #2 in W environment versus Ne, Ar and Kr concentrations: a) power to divertor plate and to the SOL; b) W concentration and Z_{eff}; c) n_e and T_e at the strike point; d) radiation fraction.

the achievement of the high deuterium densities in divertor region. Therefore, medium Z impurities (Ar, Kr) seems to be optimal seeding gasses for the low density, high power operation of the JT-60SA tokamak with W walls. The operating window, in terms of the range of the seeding gas influx, is largest for Ar seeding. Moreover, with argon seeding operations in the less optimistic situation with reduced plasma transport in the SOL (D_{SOL} $=0.25$ m^2/s) is possible. It should be noted that in case of Ne and Ar seeding, the core W radiation is always the dominant radiation loss channel, while Kr can replaces energy losses associated with the W ions in the plasma core.

4. Conclusions

The reduction of divertor target power loads due to radiation of sputtered and externally seeded impurities was investigated by means of numerical simulations of JT-60SA discharges with the COREDIV code. Calculations were performed for JT-60SA scenarios with carbon and tungsten walls assuming seeding of different gasses (N, Ne, Ar, Kr).

Carbon wall: for all scenarios considered N and C radiates predominantly in the SOL region, Ne starts to radiate also in the core, whereas Ar and Kr radiate mostly in the bulk plasma. For all scenarios with nitrogen (or Ne) seeding, gradual replacement of carbon by low Z seeding impurity is observed as the seeding gas influx increases. For the high density scenario #3 the regime of detachment on divertor plates can be achieved with N and Ne seeding. For high auxiliary power and low density scenarios, the carbon and seeding impurity radiation does not effectively reduce power to divertor and consequently, results with very high Z_{eff} (about 6-8) and impurity concentrations (≥ 9%) are observed. The use of impurities with higher atomic number does not help much but krypton might be very useful in particular when the plasma density is slightly increased. In the case of low density scenarios, increase of neither average density or edge density together with Kr seeding might lead to the development of very favorable conditions in the discharge with strong radiation losses and semi-detached conditions in the divertor.

Tungsten wall: it has been found that in both scenarios with W divertor the power delivered to the divertor plate without seeding is very high and using a seeding gas to control energy exhaust is necessary. For the scenario #3 with Ne seeding and for the reference input

parameters a wide operating window, has been found, since already for relatively low Ne concentrations ($C_{Ne} \geq 0.7$ %) the divertor heat load is below the technological limit requirements (10 MW/m^2) whereas the power crossing the separatrix stays above the P_{L-H} power threshold. The energy losses are dominated by Ne and deuterium radiation and for maximum applied seeding up to 83% of the input power can be radiated and semi-detached divertor operation can be achieved.

In case of the scenario #2, seeding by noble gasses (Ne, Ar, Kr) leads to efficient plasma cooling and tolerable heat loads to the target plates (<10 MW/m^2) at reasonable contamination level (Z_{eff}~3). Argon seems to be the optimal choice for this low density high power scenario, showing wider operating window, Ne leads to high plasma dilution at high seeding levels preventing the achievement of semi-detached conditions in the divertor. However, using krypton as a seeding gas has the advantage that it replaces tungsten in the central plasma and limits its concentration.

References

[1]   JT-60SA Research Plan - Research Objectives and Strategy Version 3.2 2015, February, *www.jt60sa.org/pdfs/JT-60SA Res Plan.pdf*

[2]   ITER Physics Expert Group on Divertor, ITER Physics Expert Group on Divertor Modelling, and Database and ITER Physics Basis Editors. Chapter 4: Power and particle control. Nucl. Fusion, **39** (12):2391, (1999)

[3]   NAKANO, T., et. al.,. Contribution of Ne ions to radiation enhancement in JT-60U divertor plasmas. J. Nucl. Materials, **438**, Supplement:S291-S296 (2013).

[4]   ZAGÓRSKI, R.,et al., Nucl. Fusion 53 (2013) 07303

[5]   ZAGÓRSKI, R., et al., "Self-consistent modeling of impurity seeded JET advanced tokamak scenarios", J. Nucl. Materials, 390-391 (2009) 404.

[6]   RAPP, J., et al., **J.** Nucl. Materials, **337-339** (2005) 826

[7]   ZAGÓRSKI, R., et al., "Integrated modelling of ASDEX upgrade nitrogen seeded discharges", Contrib. Plasma Phys. 52 (2012) 379

[8]   ZAGÓRSKI, R., et al., "Self-consistent modeling of impurity seeded JET advanced tokamak scenarios", **J.** Nucl. Materials, **390-391** (2009) 404

[9]   TELESCA, G., et al., Plasma Phys. Control. Fusion **(53),** 115002 (2011)

[10]   TELESCA, G., et al, **J.** Nucl. Materials **438**, Supplement, July 2013, S567

[11]   ZAGÓRSKI, R., et al., Nucl. Fusion 56 016018 (2016).

[12]   ZAGÓRSKI, R., et al., Contrib. to Plasma Phys.,**48**, No. 1-3 (2008) 179

[13]   MANDREKAS, J., and STACEY, W.M., Nucl. Fusion **35** (1995) 843

[14]   GARCIA, J., et al., Nucl. Fusion **54** (2014) 093010

[15]   GIRUZZI, G., et al., 2012 Model validation and integrated modelling simulations for the JT-60SA tokamak, 24th IAEA Fusion Energy Conf. (San Diego, USA, 2012) **TH/P2-03**, *http://www-naweb.iaea.org/napc/physics/FEC/FEC2012/papers/34_THP203.pdf*

[16]   LEIGHEB, M., et al., **J.** Nucl. Mater. **241-243** (1997) 914

[17]   GERHAUSER, H., et al., Nucl. Fusion **42** (2002) 805

[18]   BRAGINSKII, S.I., Rev. Plasma Phys. **1** (1965) 205

[19]   ZAGÓRSKI, R., et al., "Influence of seeding and SOL transport on plasma parameters in JET ITER-like wall H-mode discharges", **J.** Nucl. Materials, **463** (2015) 649

[20]   ZAGÓRSKI, R., et al., "Integrated core–SOL–divertor modelling for ITER including impurity: effect of tungsten on fusion performance in H-mode and hybrid scenario", Nucl. Fusion **55** (2015) 053032